Hall-Effect Sensors as Multipurpose Devices to Control, Monitor and Diagnose AC Permanent Magnet Synchronous Machines

Daniel Fernandez
Electrical Engineering Dept.
University of Oviedo
Spain
fernandezalodaniel@uniovi.es

David Reigosa
Electrical Engineering Dept.
University of Oviedo
Spain
diazdavid@uniovi.es

Yonghyun Park
Electree Co. Ltd
South Korea
yonghyun.park@eecs.korea.ac.kr

Sangbin Lee
Department of Electrical Engineering
Korea University
South Korea
sangbinlee@korea.ac.kr

Fernando Briz
Electrical Engineering Dept.
University of Oviedo
Spain
fernando@isa.uniovi.es

***Abstract*— The increasing use of permanent magnet synchronous machines is motivating the research on lower cost and higher reliability techniques for control, diagnostics and condition monitoring. Control of PMSMs typically involves current and position sensors while diagnostics tasks usually rely on vibration, flux measurements, current monitoring etc. Hall-effect sensors have shown to be a low cost, robust and reliable option for position/speed feedback (to control the machine), on-line monitoring and detection of failures through the leakage flux measurement using simple processing algorithms. This paper summarizes the available techniques for motion control, monitoring and diagnosis of permanent magnet synchronous machines using Hall-effect sensors and proposes a processing method to allow simultaneous operation of all these techniques. The output of the proposed system are estimations of the rotor position, electromagnetic torque, permanent magnet magnetization state, permanent magnet temperature and degree of eccentricity.**

Keywords—PMSM monitoring, PMSM diagnostics, PM temperature estimation, PMSM torque estimation, eccentricity detection, Hall-effect sensors

I. INTRODUCTION

Permanent magnet synchronous machines (PMSMs) drives are becoming the primary choice for traction applications in electric vehicles and hybrid-electric vehicles[1],[2]. PMSMs are being also installed in modern applications that require high torque density and a strong overload capability like more electric aircraft, satellite, etc. Due to the increasing use of PMSMs drives, accurate control, condition monitoring and diagnostics is being the focus of significant research effort since recent decades.

Instantaneous rotor position is required for the field-oriented control of PMSMs. Rotor position in PMSMs is typically measured using resolvers or encoders. However, these sensors are costly, require mechanical coupling and additional space, which compromises overall robustness of the drive. Alternatively, rotor position can be measured using linear Hall-effect sensors [3]-[15]. Hall-effect sensors can detect rotor position contactless (i.e. no mechanical couplings are required) and at a reduced cost. Different arrangements of linear Hall-effect sensors can be found in literature: two sensors, placed 90 electrical degrees apart[3][10], three sensors [11]-[14] placed 120 electrical degree apart or multiple sensors at different positions [15].

Monitoring the condition of the machine (i.e. temperature, magnetization state, eccentricity, etc.) is key to prevent rotor faults and adapt the machine operating conditions to the instantaneous limit of operation. Rotor faults are traditionally detected off-line using gaussmeter scanning, back electro-motive force (EMF) measurement, dial test indicator, and feeler gauge tests. Motor current signature analysis (MCSA) and vibration analysis are the most widespread online fault detection methods in PMSMs. However, they only work under steady-state conditions. The feasibility of using Hall-effect sensors for condition monitoring and diagnostics in PMSM drives has been also evaluated in [16]-[23]. PM temperature estimation based on the liner Hall-effect sensors has been presented in [16], PM demagnetization detection and rotor eccentricity based on linear and/or digitalized Hall-effect sensors have been presented in [16]-[20] and [20]-[22] respectively and torque estimation in PMSMs based on liner Hall-effect sensors has been presented in [23].

The justification behind the proposed Hall-effect sensor-based monitoring and diagnostics methods, and their advantages and limitations are summarized in this paper. This paper addresses all available techniques (see Table I) to control, monitor and diagnose PMSMs using Hall-effect sensors and proposes a processing method to allow simultaneous operation of all these techniques. The analysis will be done using Finite Element Analysis software (FEA) and considering a 7.5kW PMSM.

TABLE I. RELATIONSHIP BETWEEN DISCUSSED TOPICS USING HALL EFFEC SENSORS AND REFERENCES

Rotor position detection using two sensors	[3]-[10]
Rotor position detection using three sensors	[11]-[14]
Rotor position detection using ten sensors	[15]
PM temperature detection	[16]
Demagnetization detection	[17]-[20]
Eccentricity detection and load defects	[21]-[23]
Torque monitoring	[24]

This work was supported by the knowledge generation and scientific and technological strengthening Program of the Spanish Ministry of Science and Innovation under Grant MCI-20-PID2019-106057RB-I00.

This paper is organized as follows: field measurements using Hall-effect sensors is introduced in section II, Motion control of PMSM drives using Hall-effect sensors is discussed in section III, monitoring of PMSMs using Hall-effect sensors is discussed in section IV, the use of hall effect sensors for diagnostics is explained in section V, FEA simulation results are presented in section VI and finally, conclusions are presented in section VII.

II. Field Measurements Using Hall-Effect Sensors

In conventional PMSM drives equipped with Hall-effect sensors, they are attached to the stator or the end shield of the machine [3]-[23] in order to measure PM leakage flux. Linear motor systems equipped with Hall-effect sensors place them on the mover, facing the PMs [14]. Fig. 1 shows an example of the PM leakage flux distribution of a conventional IPMSM (i.e. radial flux machine) obtained using FEA and the approximate position of the Hall-effect sensors.

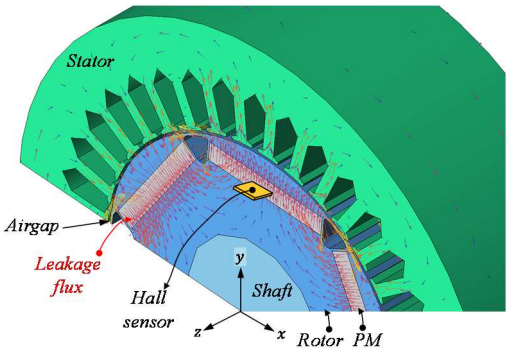

Fig. 1. FEA results. Leakage flux vectors on an IPMSM machine and location of a Hall-effect sensor.

At the measuring point, the flux vector can be decomposed into three components, see Fig. 1: *x*-axis component (tangential), *y*-axis component (radial) and *z*-axis component (axial). Any of them can be potentially used for machine drive control, monitoring or diagnostics. However, the axial component typically provides the weakest signal [13] and does not contain useful information for torque estimation purposes [23] so it is often neglected.

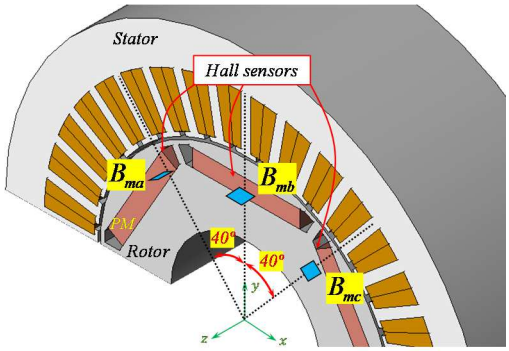

Fig. 2. Hall-effect sensors position for a six-pole machine using three Hall-effect sensors

Fig. 2 shows the position of the three Hall-effect sensors, B_{ma}, B_{mb} and B_{mc} inside a six-pole IPMSM. The IPMSM main characteristics and dimensions are listed in Table II. The Hall-effect sensors are placed 5mm away from the magnets edge (z-axis), and at 51 mm from the shaft center (y-axis), matching the position of the magnets from the shaft center. The mechanical angle among sensors is 40 mechanical degrees resulting in 120 electrical degrees for a six-pole machine.

TABLE II. Machine Parameters And Main Dymensions

Rated power	7.5	kW
Rated Current	14	A
Number of Poles	6	
Rated Speed	1800	rpm
Outer diameter	180	mm
Rotor diameter	110	mm
Airgap length	0.8	mm
Magnet position	54	mm
Magnet width	42	mm
Magnet thickness	6	mm
Magnet type	N42SH	

An example of the three components of the flux, *xyz* obtained at the same measurement point for a complete electrical cycle is shown in Fig. 3a. It can be observed that the *y*-axis component (radial) is the most sensitive and the most sinusoidal component. Fig. 3b shows the *y*-axis component of the leakage flux when three sensors, B_{ya}, B_{yb} and B_{yc}, are used (see Fig. 2b).

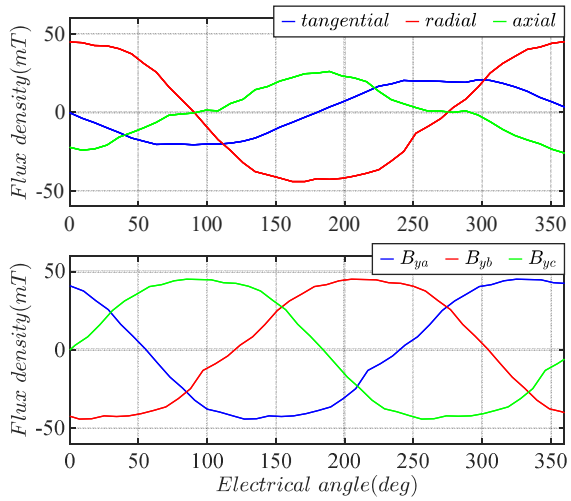

Fig. 3. Measured flux density waveforms a) tangential, radial and axial components at the same location b) tangential component at three different locations using three sensors (Fig. 2).

Measurement of leakage flux in PMSMs allow their control, monitoring and diagnostics (see Table I). Fig. 4 shows the proposed processing system to allow simultaneous on-line parameter estimation using Hall-effect sensors. Complex vector is used for rotor position, speed and electromagnetic torque estimation; demagnetization is detected using patter comparison; digitalized signal is used for rotor eccentricity and demagnetization detection; rotor temperature is obtained from the RMS value of a leakage flux waveform. These techniques will be described in the following sections.

III. Motion Control Of PMSM Drives Using Hall-Effect Sensors

Leakage flux in stationary reference frame contains information of the rotor position [3]-[15]. When three Hall-

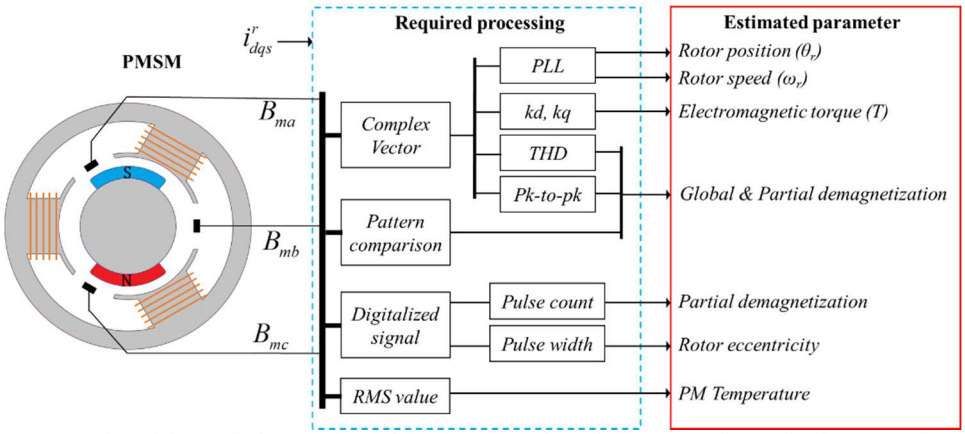

Fig. 4. Schematic representation of the required processing and simultaneous estimated parameters using Hall-effect sensors in PMSMs.

effect sensors are used, a complex vector $\overline{B}^s_{mdqs}$ can be defined according to (1), where B_{ma}, B_{mb} and B_{mc} are the m component (x, y or z) of the leakage flux density, B, measured at three different locations a, b and c, 120 degrees apart.

$$\overline{B}^s_{mdqs} = 2/3(B_{ma} + aB_{mb} + a^2 B_{mc}) \quad (1)$$

Once the complex vector in stationary reference frame is obtained (1), a Phase Lock Loop (PLL), can be used to obtain the rotor speed and position [5], [7].The main limitations of the available methods to extract the rotor position are the bandwidth, due to the PLL dynamics, and the accuracy compared to encoders or resolvers. Fig. 5 shows the schematic representation of a synchronous reference frame PLL used for the estimation of rotor speed and position in this paper. The d and q axis leakage flux density, B^s_{mds} and B^s_{mqs} in stationary reference frame are normalized and rotated to synchronous reference frame using the estimated rotor position $\hat{\theta}_r$. A PI synchronous regulator is used in the PLL, see Fig. 5, to cancel out the error resulting of subtracting the signal B^r_{mqs} to a zero reference.

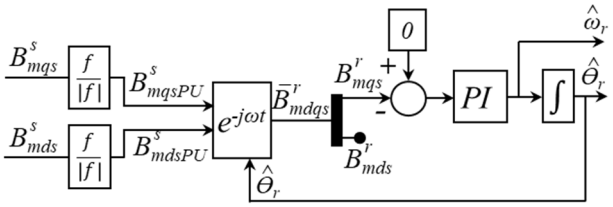

Fig. 5. Block diagram of the synchronous reference frame PLL algorithm, for Hall-sensor based rotor position and speed estimation using Hall-effect sensors.

IV. Monitoring Of PMSM Drives Using Hall-Effect Sensors

A. PM Temperature estimation

According to [16], PM temperature in PMSMs can be estimated using three linear Hall-effect sensors attached to the end shield of the machine. Assuming that the relationship between the PM flux, $B(T_{PM})$, and the PM temperature, T_{PM}, is given by (2), where T_{PM} and T_{PM0} are the present and reference PM temperatures and α_{PM} is the thermal coefficient of flux density of the PM material, PM temperature can be estimated. As the Hall-effect sensors produce a voltage proportional to the applied flux B, leakage flux produced by armature currents can lead to high estimation errors. However, this effect can be decoupled when the instantaneous armature current is available for the temperature estimation algorithm [16], as shown in Fig. 4. Fig. 6 shows the block diagram of the proposed algorithm for the Hall-sensor based PM temperature estimation. The magnitude of the complex vector is calculated, a compensation signal is applied as function of the armature current. Using (2) and having the reference values for flux and temperature and α_{PM}, estimated PM temperature can be obtained.

$$B(T_{PM}) = B(T_{PM0}) \cdot (1 + \alpha_{PM} \cdot (T_{PM} - T_{PM0})) \quad (2)$$

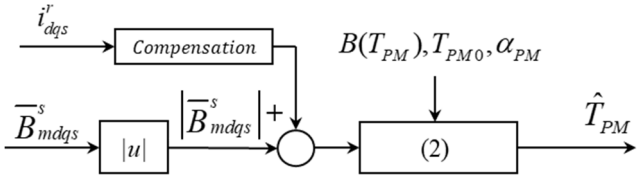

Fig. 6. Block diagram of the algorithm for Hall-sensor based PM temperature estimation.

B. Torque Monitoring

The complex vector of the leakage flux (1) is also used in [24] to estimate the PMSM torque of a surface and an interior PMSM. The method assumes that the PMSM flux linkages λ^r_{ds} and λ^r_{qs} behaves similarly in stator and rotor cores. Radial and tangential leakage flux components, λ^r_{lds} and λ^r_{lqs} are given by the interaction of the coil flux and permanent magnet flux and can be measured using Hall effect sensors.

$$T = \frac{3p}{2}(\lambda^r_{ds} i^r_{qs} - \lambda^r_{qs} i^r_{ds}) \quad (3)$$

$$\hat{T} = \frac{3p}{2}(k_d B^r_{lds} i^r_{qs} - k_q B^r_{lqs} i^r_{ds}) \quad (4)$$

Total torque developed by a PMSM is given by (3), where i^r_{ds} and i^r_{qs} are the d- and q- axes currents in a reference frame

$$k_d = \frac{\lambda^r_{ds}}{B_{lds}} \quad (5)$$

$$k_q = \frac{\lambda^r_{qs}}{B_{lqs}} \quad (6)$$

synchronous with the rotor and p is the number of pole pairs. According to [23], machine torque can also be approximated as in (4), see Fig. 7, where k_d and k_q are coefficients that link the stator flux linkage, $\bar{\lambda}_{ldqs}$, and the leakage flux density, $\bar{B}^r_{ldqs}$, measured by the Hall-effect sensors. The coefficients k_d and k_q are deefiend by (5) and (6). This coefficients are depedent on the operating conditions and are experimentally estimated in [23] for the whole *Idq* map. However, for some operating regions on the map, k_d and k_q are averaged as costants as its variation can be negligible.

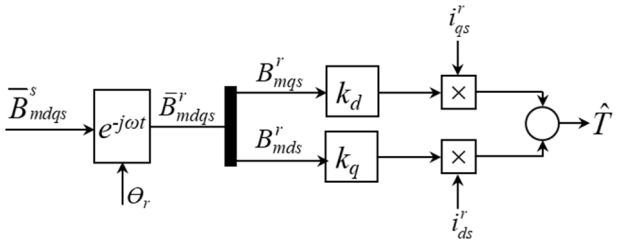

Fig. 7. Block diagram of the algorithm for Hall-sensor based PMSM torque estimation.

V. Diagnostics Of PMSM Drives Using Hall-Effect Sensors

A. Demagnetization Detection

Global and partial (local) demagnetization can be detected by analyzing the peak-to peak and mean values of the zero sequence of the magnetic flux density measurements [19]. The zero-sequence magnetic flux density vector, B_{mdq0}, can be defined as (7). This signal will be periodic for a mechanical revolution and will reflect asymmetries of the magnetic flux density measured by the Hall effect sensors, B_{ma}, B_{mb} and B_{mc}.

$$B_{mdq0} = 1/3(B_{ma} + B_{mb} + B_{mc}) \quad (7)$$

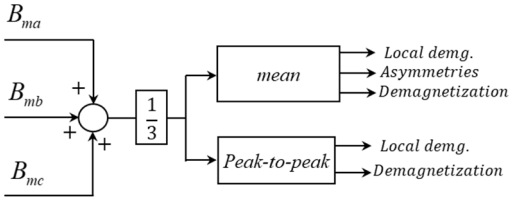

Fig. 8. Block diagram of the algorithm for Hall-sensor based demagnetization detection in PMSMs according to [19].

Global and partial demagnetization can also be detected using only one Hall-effect sensor as in [20]. Fig. 8 shows a block diagram of the required algorithm, where the magnetic flux density provided by one Hall-effect sensor is rectified (absolute value) and compared to a threshold value. The resulting digital signal is of variable pulse width when asymmetries in the leakage flux occur. The pulse width and the pulse count will depend on the level of eccentricity and demagnetization. Local demagnetization will reduce the pulse count for a mechanical period and the degree of eccentricity will vary the pulse width of all pulses for a mechanical revolution [20].

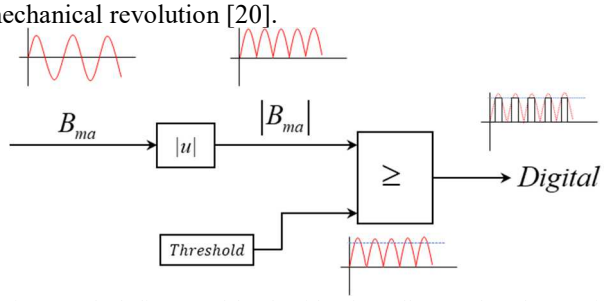

Fig. 9. Block diagram of the algorithm for Hall-sensor based eccentricity and demagnetization detection in PMSMs according to [20].

B. Detection of eccentricity and load defects

Mechanical defects or imperfections in PMSM systems produce vibration at the fundamental frequency leading to oscillation in the load torque at rotor speed [21]. Load unbalance, misalignment, load eccentricities, mechanical looseness, mechanical wear, turbulence in flow, load fluctuation, etc. produces oscillation at the fundamental frequency [21]. Unlike PMSM rotor defects, these imperfections do not have any influence on the amplitude of the Hall sensor flux measurements since the rotor MMF or airgap does not change with coupling or load defects. However, if static, dynamic, or mixed eccentricity is present in the rotor, the airgap changes with rotor position resulting in variations in the peak values of the PM leakage flux.

Using only one Hall-effect sensor (B_{ma}, B_{mb} or B_{mc}) local demagnetization, load defects and eccentricity can be detected, see Fig. 10, and reliably separated if these phenomena coexist. In addition, it can be detected during transients.

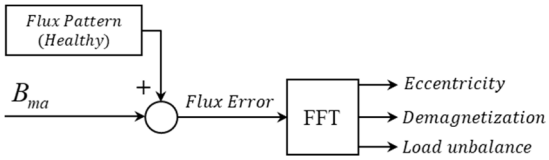

Fig. 10. Block diagram of the algorithm for Hall-sensor based PMSM eccentricity, demagnetization and load unbalance detection.

VI. FEA Simulation Results

Fig. 11 shows the FEA results obtained for a 7.5 kW machine, see Table II for a total time of 10s and for a rotor speed of 600 rpm.

Fig. 11a shows the resulting leakage flux measurement of the IPMSM under different operating conditions: at t=0s PM temperature is configured in the simulation to vary from 20 to 60ºC with the machine unloaded; an Iq current step of 14 A (rated current) is performed at t=3.4 s keeping PM temperature constant at 60ºC; the IPMSM is unloaded at t=6.6s and a partial demagnetization of 10% is emulated in one PM for this last period. It can be observed in Fig. 5a that the measured leakage flux for the three Hall-effect sensors, B_{ya}, B_{yb} and B_{yc} is slightly reduced, in terms of peak-to-peak-value as PM temperature increases. The peak-to-peak value is also affected by the armature current as it can be observed in Fig. 11a for the period 3.4 to 6.6s.

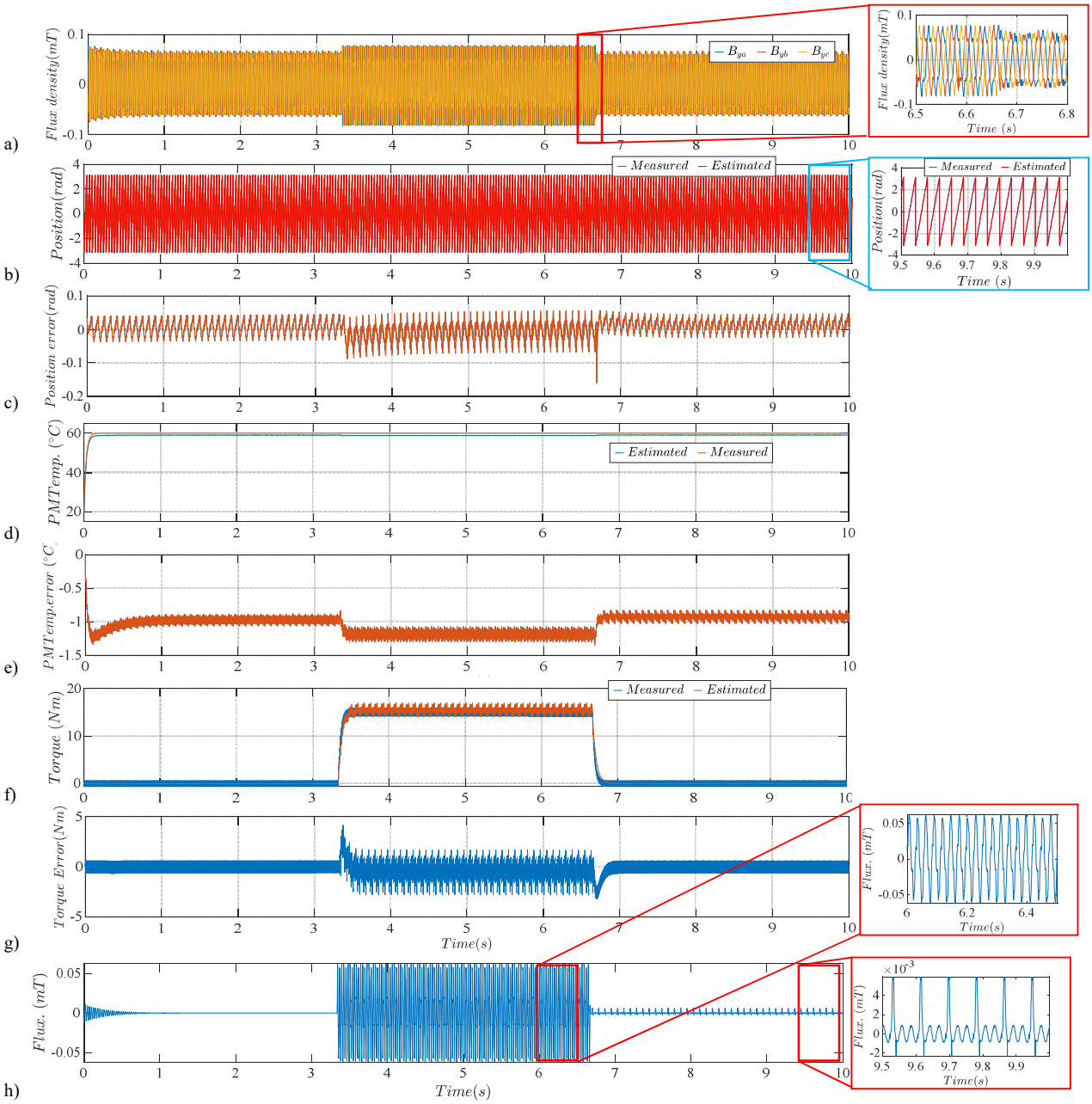

Fig. 11. FEA results: a)Leakage flux measurement, b) estimated rotor position, c) error of the estimated rotor position, d)estimated PM temperature, e) PM temperature estimation error, f)estimated torque, g) estimated torque error and h) differential flux for partial demagnetization detection. Rotor speed is 600 rpm.

Fig. 11b shows the estimated position using the complex vector and a synchronous reference frame PLL [13], see Fig. 5. It can be observed in the estimated position error, Fig. 11c, that the estimated position is barely affected by the PM temperature, or armature current since these effects only alter the peak-to-peak value of the waveforms and the complex vector is normalized at the input of the PLL, see Fig. 5.

PM temperature can be obtained on-line under any operating conditions of the machine as shown in Fig. 11d, using the signal processing detailed in Fig. 6. Since PM temperature is detected using the RMS value of the complex flux vector, any change in the magnitude of the leakage flux produced by armature currents can lead to high estimation errors, see Fig. 11e from t=3.4s to t=6.6s. Armature currents produce the largest changes in the magnitude of the complex vector, as shown in Fig. 11a. However, this phenomenon can be decoupled if the armature currents are available for the control system.

Fig. 11f. shows the FEA results of the torque estimation method using Hall-effect sensors [23] with constant k_d and k_q. Under these conditions the estimation error is ±3Nm, as it can be observed in Fig. 11g. Note that the rated torque delivered by this machine is 44Nm. The error can be reduced if dynamic values of k_d and k_q are used.

Fig. 11h shows the error leakage flux of one Hall-effect sensor (i.e. measured flux subtracted to the expected flux at a given PM temperature) of a 6 pole PMSM with one magnet partially demagnetized (MS of one magnet configured to 90%) at t=6.6s. It can be observed that the mean value of the signal is approximately zero for the period from t=0 to t=6.6s. When the partial demagnetization is introduced, t=6.6s, a peak per rotor revolution arises producing an average value

of the signal different from zero, which is a clear indication of local PM demagnetization.

VII. Conclusions

This paper summarizes available techniques to control, monitor the condition, and detect of faults in PMSMs using only linear Hall-effect sensors and proposes a method to allow simultaneous operation of all these techniques. It is shown that these techniques represent an economical and powerful tool for the controllability and reliability of PMSM drives. The main aspects of the techniques surveyed include the rotor position detection, PM temperature estimation, detection of rotor (demagnetization and eccentricity) and load defects, and torque monitoring. An extended analysis of each individual estimation method has been evaluated and the accuracy of estimation has been also evaluated using FEA.

References

[1] J. Lara, J. Xu and A. Chandra, "Effects of Rotor Position Error in the Performance of Field-Oriented-Controlled PMSM Drives for Electric Vehicle Traction Applications," in IEEE Transactions on Industrial Electronics, vol. 63, no. 8, pp. 4738-4751, Aug. 2016, doi: 10.1109/TIE.2016.2549983.

[2] Z. Q. Zhu and D. Howe, "Electrical Machines and Drives for Electric, Hybrid, and Fuel Cell Vehicles", Proc. IEEE, vol. 95, no. 4, pp. 746–765, Apr. 2007, doi: 10.1109/JPROC.2006.892482.

[3] Q. Zhu, Y. F. Shi, and D. Howe, "Rotor position sensing in brushless ac motors with self-shielding magnets using linear Hall sensors," J. Appl. Phys., vol. 99, no. 8, pp. 08R 313–08R 313-3, Apr. 2006.

[4] [4]. L. Xiao, Y. Yunyue, and Z. Zhuo, "Study of the linear Hall-effect sensors mounting position for PMLSM," in Proc. IEEE ICIEA, May 2007, pp. 1175–1178.

[5] [5]. S. Jung and K. Nam, "PMSM Control Based on Edge-Field Hall Sensor Signals Through ANF-PLL Processing," in IEEE Transactions on Industrial Electronics, vol. 58, no. 11, pp. 5121-5129, Nov. 2011, doi: 10.1109/TIE.2011.2116850.

[6] Phuong Thi Luu, Ji-Young Lee, Ji-Won Kim, Shi-Uk Chung, Soon-Man Kwon, "Magnetic Sensor Design for a Permanent Magnet Linear Motor Considering Edge-Effect", Industrial Electronics IEEE Transactions on, vol. 67, no. 7, pp. 5768-5777, 2020.

[7] Xiaojiang Chen, Adam Pride and Shinichiro Iwasaki, "Permanent magnet synchronous motor and controller therefor", U.S. Patent: US7714529B2, May 2004.

[8] F. Giulii Capponi, G. De Donato, L. Del Ferraro, O. Honorati, M. C. Harke and R. D. Lorenz, "AC brushless drive with low-resolution Hall-effect sensors for surface-mounted PM Machines," in IEEE Transactions on Industry Applications, vol. 42, no. 2, pp. 526-535, March-April 2006, doi: 10.1109/TIA.2005.863904.

[9] D. Fernandez, D. Fernandez, M. Martinez, D. Reigosa, A. B. Diez and F. Briz, "Resolver Emulation for PMSMs Using Low Cost Hall-Effect Sensors," in IEEE Transactions on Industry Applications, vol. 56, no. 5, pp. 4977-4985, Sept.-Oct. 2020, doi: 10.1109/TIA.2020.3008129.

[10] X. Song, J. Fang and B. Han, "High-Precision Rotor Position Detection for High-Speed Surface PMSM Drive Based on Linear Hall-Effect Sensors," in IEEE Transactions on Power Electronics, vol. 31, no. 7, pp. 4720-4731, July 2016, doi: 10.1109/TPEL.2015.2479642.

[11] F. Caricchi, F. G. Capponi, F. Crescimbini, and L. Solero, "Sinusoidal brushless drive with low-cost linear Hall effect position sensors," in Proc. IEEE Power Electron. Spec. Conf., Jun. 2001, vol. 2, pp. 799–804.

[12] R. Wegener, F. Senicar, C. Junge, and S. Soter, "Low cost position sensor for permanent magnet linear drive," in Proc. IEEE PEDS, Nov. 2007, pp. 1367–1371.

[13] D. Reigosa, D. Fernandez, C. González, S. B. Lee and F. Briz, "Permanent Magnet Synchronous Machine Drive Control Using Analog Hall-Effect Sensors," in IEEE Transactions on Industry Applications, vol. 54, no. 3, pp. 2358-2369, May-June 2018, doi: 10.1109/TIA.2018.2802950.

[14] J. Kim, S. Choi, K. Cho and K. Nam, "Position Estimation Using Linear Hall Sensors for Permanent Magnet Linear Motor Systems," in IEEE Transactions on Industrial Electronics, vol. 63, no. 12, pp. 7644-7652, Dec. 2016, doi: 10.1109/TIE.2016.2591899.

[15] Y. Wang, Y. Hoole and K. Haran, "Position Estimation of Outer Rotor PMSM Using Linear Hall Effect Sensors and Neural Networks," 2019 IEEE International Electric Machines & Drives Conference (IEMDC), San Diego, CA, USA, 2019, pp. 895-900, doi: 10.1109/IEMDC.2019.8785178.

[16] D. Fernandez, et al., "Permanent magnet temperature estimation in PM synchronous motors using low-cost Hall effect sensors," IEEE Trans. Ind. Appl., vol. 53, no. 5, pp. 4515-4525, Sept./Oct. 2017.

[17] S. Attestog, H. Van Khang and K. G. Robbersmyr, "Modelling Demagnetized Permanent Magnet Synchronous Generators using Permeance Network Model with Variable Flux Sources," 2019 22nd International Conference on the Computation of Electromagnetic Fields (COMPUMAG), Paris, France, 2019, pp. 1-4, doi: 10.1109/COMPUMAG45669.2019.9032791.

[18] D. Reigosa, D. Fernández, Y. Park, A. B. Diez, S. B. Lee and F. Briz, "Detection of Demagnetization in Permanent Magnet Synchronous Machines Using Hall-Effect Sensors," in IEEE Transactions on Industry Applications, vol. 54, no. 4, pp. 3338-3349, July-Aug. 2018, doi: 10.1109/TIA.2018.2810123.

[19] D. Reigosa, et al., "Permanent magnet synchronous machine non-uniform demagnetization detection using zero-sequence magnetic field density," IEEE Trans. Ind. Appl., vol. 55, no. 4, pp. 3823-3833, July/Aug. 2019.

[20] Y. Park, et al., "Online detection of rotor eccentricity and demagnetization faults in PMSMs based on Hall-effect field sensor measurements," IEEE Trans. Ind. Appl., vol. 55, no. 3, pp. 2499-2509, May/June 2019.

[21] Y. Park, et al., "Online detection and classification of rotor and load defects in PMSMs based on Hall sensor measurements," IEEE Trans. Ind. Appl., vol. 55, no. 4, pp. 3803-3812, July/Aug. 2019.

[22] Zihao Xu, Kunxi Qian and Hao Wang, "Measurement of permanent maglev turbine's rotor eccentricity by Hall sensors," 2010 International Conference on Computer, Mechatronics, Control and Electronic Engineering, Changchun, 2010, pp. 100-103, doi: 10.1109/CMCE.2010.5610370.

[23] D. F. Alonso, Y. Kang, D. F. Laborda, M. M. Gómez, D. D. Reigosa and F. Briz, "Permanent Magnet Synchronous Machine Torque Estimation Using Low Cost Hall-Effect Sensors," 2019 IEEE 10th International Symposium on Sensorless Control for Electrical Drives (SLED), Turin, Italy, 2019, pp. 1-6, doi: 10.1109/SLED.2019.8896292.

[24] J. Hong, S.B. Lee, C. Kral, and A. Haumer, "Detection and Classification of Rotor Demagnetization and Eccentricity Faults for PM Synchronous Motors," IEEE Trans. on Ind. Appl., vol. 48, no. 3, pp. 923-932, May/June 2012.